

# Line-images in Cone Mirror Catadioptric Systems

J. Bermudez-Cameo, G. Lopez-Nicolas and J.J. Guerrero  
Instituto de Investigación en Ingeniería de Aragón (I3A)  
Departamento de Informática e Ingeniería de Sistemas  
Universidad de Zaragoza, Spain

**Abstract**—The projection surface of a 3D line in a non-central camera is a ruled surface, containing the complete information of the 3D line. The resulting line-image is a curve which contains the 4 degrees of freedom of the 3D line. In this paper we investigate the properties of the line-image in conical catadioptric systems. This curve is a particular quartic that can be described by only six homogeneous parameters. We present the relation between the line-image description and the geometry of the mirror. This result reveals the coupling between the depth of the line and the distance from the camera to the mirror. If this distance is unknown the 3D information of a projected line can be recovered up to scale. Knowing this distance allows obtaining the 3D metric reconstruction. The proposed parametrization also allows to simultaneously reconstruct the 3D line and computing the aperture angle of the mirror from five projected points on the line-image. We analytically solve the metric distance from a point to a line-image and we evaluate the proposal with real images.

## I. INTRODUCTION

In central systems the projection of a 3D line is a plane passing through the 3D line and the viewpoint of the camera which helps the line-image extraction [1]. In this class of projection some of the information of the 3D line is lost because any line lying on this plane is projected on the same line-image. In other words, a 3D line occludes any other line located behind because the projection surface is a plane.

By contrast, in non-central systems the projecting rays do not intersect a common viewpoint. The locus of the viewpoint is in general tangent to a caustic [2] which is an envelope surface of the projecting rays. When the system is axial each projecting ray is defined by a 3D point and the intersection of the ray with an axis which is the axis of symmetry if the system has revolution symmetry. The projecting rays coming from a 3D line are skew 3D lines forming a ruled surface which lies on the axis of symmetry. In [3] it is proven that four generic lines<sup>1</sup> induce two incident lines. Therefore, when we have a surface defined by at least four skew (and non cohyperbolic) rays only two lines intersecting all the rays lie on this surface. In this case, is it possible to occlude a 3D line with other line? The previous result implies that the projection surface contains the axis of revolution, the given line and any line intersecting both the axis and the line. No additional line can belong to this surface, hence lines do not occlude other lines in non-central projections.

As a consequence, the complete geometry of a 3D line is mapped on a single non-central image and it can be completely

<sup>1</sup>Four lines are generic if no two of them are coplanar, no three of them are coconical or cocylindrical, and the four are not cohyperbolic, i.e. do not lie on the same ruled quadric surface.

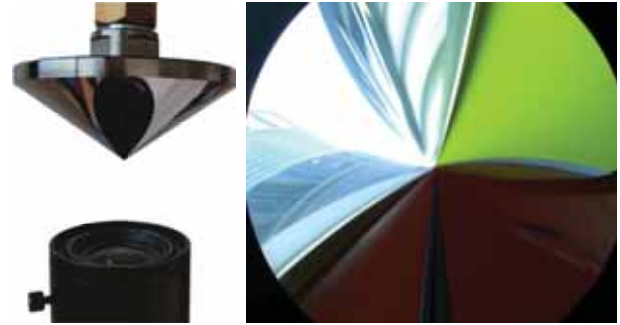


Fig. 1. An image taken with a conical catadioptric system.

recovered from at least 4 line-image points or projecting rays [4], [5], [6]. On the contrary, points do not provide 3D information since points always occlude other points.

A simple non-central system can be built using a cone mirror (conical catadioptric mirrors). In general, these systems are non-central and they can be axial if the camera is located at the axis of revolution or off-axis when the camera is out of this axis. Figure 1 shows a conical catadioptric mirror and an image taken with this system.

Some previous approaches have tried to extract 3D lines from a single image in non-central catadioptric systems. In [6], [4] 3D lines are defined from 4 rays comparing different computation approaches. One of them is based on the intersection between a ray and the line which is encoded using the side operator between Plücker coordinates of lines. The other approach is based on the intersections of surfaces defined by two sets of 3 rays. Some simplifications have been used to improve the reconstructions by reducing the DOFs of the problem considering only horizontal lines [7] [8] or exploiting cross-ratio properties [9].

Line projections have been also used to estimate the calibration of non-central systems in a generalization of the plum line approach. In [10] non-central calibration using lines is studied. They exploit the fact that there exist less ambiguity when the system is off-axis with impressive results. However, this work does not exploit the particular geometric description of the line-images. In [11] they exploit particular geometric properties of spherical mirrors for computing extrinsic calibration parameters but they do not use lines.

In this paper, we present a new compact description of the line-image (projection of a straight line) in conical catadioptric images. This description allows to fit the projection of straight lines linearly without knowing the extrinsic calibration

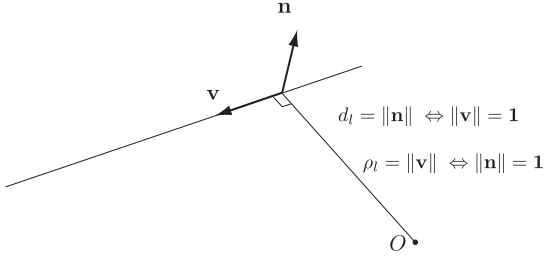


Fig. 2. Euclidean interpretation of Plücker coordinates.

parameters of the system (the aperture angle of the mirror and the distance to the mirror). We also solve in close form the metric distance from point to line-image in conical catadioptric images and we propose it to fit and extract these projections.

In Section II we introduce the necessary background to understand the proposal. In Section III we present the proposed description of the line-image for conical catadioptric systems. In Section IV we analytically solve the metric distance from a point to the line-image. In Section V we evaluate the method with real images. Finally in Section VI we present the conclusions.

## II. BACKGROUND

### A. Plücker coordinates

The Plücker coordinates of a 3D line is an homogeneous representation of a line  $l \in \mathbb{P}^5$  defined by the null space of two  $\mathbb{P}^3$  points of the line. When correctly arranged, this representation can be decomposed in two  $\mathbb{R}^3$  vectors  $\mathbf{l} = (\mathbf{v}, \mathbf{n})^T$  with geometrical meaning in Euclidean geometry.  $\mathbf{v} \in \mathbb{R}^3$  is called the direction vector and represents the direction of the line.  $\mathbf{n} \in \mathbb{R}^3$  is called the moment vector and represents the normal to a plane passing through the 3D line and the reference system  $O$ . Not all elements of  $\mathbb{P}^5$  correspond to 3D lines. Any point of  $\mathbb{P}^5$  corresponding to a line in  $\mathbb{P}^5$  must satisfy  $\mathbf{v}^T \mathbf{n} = 0$  which is known as Plücker identity.

The Euclidean interpretation is the orthogonality between the direction and the projection plane  $\mathbf{n}$  (see Figure 2). When the homogeneous vector  $\mathbf{l}$  is normalized with respect to the norm of  $\mathbf{v}$ ,  $\|\mathbf{n}\| = d_l$  where  $d_l$  is the minimum distance from the origin  $O$  to the 3D line. We call this description *direct normalized representation* of a Plücker line. On the contrary, when it is normalized respect to the norm of  $\mathbf{n}$ ,  $\|\mathbf{v}\| = \rho_l$  where  $\rho_l$  is the inverse to this distance. We call this description *inverse normalized representation* of a Plücker line.

### B. Conical Mirror Systems

In conical catadioptric systems with the camera located in the axis of revolution of the mirror, the locus of viewpoint is a circle of radius  $R_c$  centred in the vertical axis at height  $Z_c$  [12], [13]. The locus of this circle, which depends on the distance  $Z_m$  between the camera and the vertex of the mirror and the aperture angle  $\tau$  of the mirror, is

$$R_c = Z_m \sin 2\tau \quad , \quad Z_c = Z_m (1 - \cos 2\tau) . \quad (1)$$

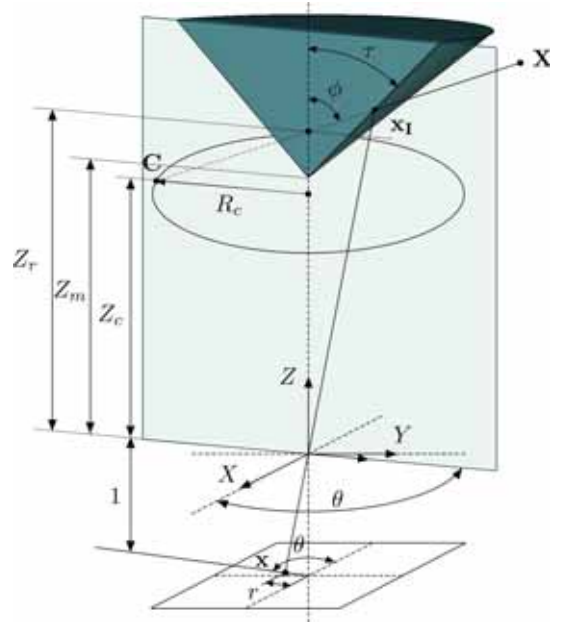


Fig. 3. Conical catadioptric projection of a point  $\mathbf{X}$ .

*a) The forward projection model:* As the viewpoint locus is a circle and there exist a revolution symmetry the forward projection is unambiguous and direct. Given a 3D point  $\mathbf{X} = (X_1, X_2, X_3, X_4)^T \in \mathbb{P}^3$  in the camera reference, the non-central projection ray is contained in a plane containing the axis of revolution of the mirror. The intersection of this plane with the circle is a single point  $C$ , therefore the projection ray is completely defined by  $\mathbf{X}$  and  $C$ . The intersection of this line with the mirror gives the point  $x_I$  which is projected in point  $\mathbf{x} \in \mathbb{P}^2$  on the normalized plane.

$$x = \left( \sin 2\tau \frac{(X_3 - Z_m X_4)}{\sqrt{X_1^2 + X_2^2}} - \cos 2\tau \right) X_1 \quad (2)$$

$$y = \left( \sin 2\tau \frac{(X_3 - Z_m X_4)}{\sqrt{X_1^2 + X_2^2}} - \cos 2\tau \right) X_2 \quad (3)$$

$$z = Z_m X_4 + (X_3 - Z_m X_4) \cos 2\tau + \sqrt{X_1^2 + X_2^2} \sin 2\tau \quad (4)$$

This projection is related to the image plane with a perspective camera model involving a linear transformation and a distortion model.

We use the matrix  $K_c$  to transform the coordinates of the normalized plane  $(x, y, z) \in \mathbb{P}^2$  to the image coordinates  $(u, v) \in \mathbb{R}^2$ . The principal point  $(u_0, v_0)$  corresponds to the vertex cone projection.

$$\begin{pmatrix} u \\ v \\ 1 \end{pmatrix} \sim \underbrace{\begin{pmatrix} f_x & s_{skew} & u_0 \\ 0 & \pm f_y & v_0 \\ 0 & 0 & 1 \end{pmatrix}}_{K_c} \begin{pmatrix} x \\ y \\ z \end{pmatrix} \quad (5)$$

b) *The back projection model:* In a general non-central system each ray is defined by two points [14], e.g. the 3D point and a point in which the ray is tangent to a surface called caustic. When the system has symmetry of revolution any ray can be expressed in terms of three parameters: elevation angle  $\phi$ , azimuth angle  $\theta$  and distance to the intersection between the ray and the vertical axis  $Z_r$  (see Figure 3). The representation of this ray in Plücker coordinates is

$$\mathbf{l}_{ray} = \begin{pmatrix} \mathbf{v}_{ray} \\ \mathbf{n}_{ray} \end{pmatrix} = \begin{pmatrix} \sin \phi \cos \theta \\ \sin \phi \sin \theta \\ \cos \phi \\ Z_r \sin \phi \sin \theta \\ -Z_r \sin \phi \cos \theta \\ 0 \end{pmatrix}. \quad (6)$$

Notice that, when taking polar coordinates ( $r = \sqrt{x^2+y^2}$  and  $\theta = \text{atan2}(y, x)$ ) in this reference,  $\theta$  corresponds to the azimuth angle shown in the ray description. The elevation angle  $\phi$  and  $Z_r$  depend on image radius  $r$  and the system calibration.

In particular, for the case of a conical catadioptric system  $Z_r$  depends on  $\cot \phi$

$$Z_r = Z_c + R_c \cot \phi \quad (7)$$

which is related with  $r$  by

$$\cot \phi = \frac{1 + r \tan 2\tau}{\tan 2\tau - r}. \quad (8)$$

### C. Lines in non-central systems

Given a 3D line expressed in Plücker coordinates  $\mathbf{l} = (\mathbf{v}_l, \mathbf{n}_l)^\top = (v_x, v_y, v_z, n_x, n_y, n_z)^\top$ , a projecting ray  $\mathbf{l}_{ray}$  intersects the line when

$$\text{side}(\mathbf{l}, \mathbf{l}_{ray}) = \mathbf{n}_{ray}^\top \mathbf{v}_l + \mathbf{n}_l^\top \mathbf{v}_{ray} = 0 \quad (9)$$

where the side operator is the intersecting constraint for Plücker lines.

The resulting linear system obtained from this constraint with at least four rays is used in [3] and [6] to compute the Plücker representation of the 3D line. As Plücker coordinates are over-parametrized the null space of the solution has one dimension. However, not all six-elements vector corresponds to a Plücker line. By imposing the Plücker line constraint ( $\mathbf{v}^\top \mathbf{n} = 0$ ) two solutions are obtained. One is the axis of symmetry and the other is the sought line. Notice that there exist some degenerated central cases in which projecting surfaces are planes (called Planar Viewing Surfaces (PVS) in [6]) and the geometry of the 3D line cannot be recovered. These degenerated cases are: the Axial-PVS case when the line is coplanar with the axis of symmetry and the Horizontal-PVS case when all the projecting rays lie in an horizontal plane ( $\phi = \frac{\pi}{2}$ ).

## III. LINE-IMAGES IN CONICAL MIRROR SYSTEMS

A line-image is a curve on a two dimensional projected space which defines the collection of rays intersecting a 3D line. This curve is obtained by placing the back-projection model in equation (9). Generalizing the framework used in [15] to non central systems, the general expression for a line-image in non-central systems is

$$Z_r (v_x y - v_y x) + (n_x x + n_y y) + n_z z r \cot \phi = 0. \quad (10)$$

With at least 4 points of the line-image we can compute the 3D line in a direct way by solving the linear system

$$\begin{pmatrix} Z_{r_i} y_i & -Z_{r_i} x_i & x_i & y_i & z_i r_i \cot \phi_i \end{pmatrix} \tilde{\mathbf{l}} = 0 \quad (11)$$

where  $\tilde{\mathbf{l}} = (v_x, v_y, n_x, n_y, n_z)^\top$  for  $i = 1, \dots, 4$ .

Notice that in this case  $v_z$  has disappeared from the equation and we are obtaining an element of  $\mathbb{P}^4$ , therefore the null space is a single solution instead of the one dimension space obtained when solving with (9) in [3]. Actually, the Plücker identity used to reduce this space in [3] is used here to compute  $v_z$  due to the redundancy of Plücker coordinates representation.

When particularizing these expressions to the conical catadioptric system, this line image can be developed to a polynomial expression of degree 4 (a quartic described by 15 monomials in general). However, when the equation is expressed in polar coordinates this expression can be written in a compact form with 6 parameters encapsulating the Plücker coordinates of the line and the mirror parameters of the system. The line-image is then written as

$$\begin{pmatrix} r \cos \theta & r \sin \theta & r & \cos \theta & \sin \theta & 1 \end{pmatrix} \boldsymbol{\omega} = 0 \quad (12)$$

where

$$\boldsymbol{\omega} = \begin{pmatrix} \omega_1 \\ \omega_2 \\ \omega_3 \\ \omega_4 \\ \omega_5 \\ \omega_6 \end{pmatrix} = \begin{pmatrix} -\frac{1-\cos 2\tau}{\cos 2\tau} Z_m v_y - n_x \\ \frac{1-\cos 2\tau}{\cos 2\tau} Z_m v_x - n_y \\ n_z \tan 2\tau \\ \tan 2\tau (n_x - Z_m v_y) \\ \tan 2\tau (n_y + Z_m v_x) \\ n_z \end{pmatrix}. \quad (13)$$

This expression allows us to linearly compute the line-image from five points without knowing neither the aperture angle of the mirror  $\tau$  nor the distance to the mirror  $Z_m$ , by solving

$$\begin{pmatrix} r_i x_i & r_i y_i & z_i r_i^2 & x_i & y_i & z_i r_i \end{pmatrix} \boldsymbol{\omega} = 0 \quad (14)$$

for  $i = 1, \dots, 5$ .

Once the line-image  $\boldsymbol{\omega} \in \mathbb{P}^5$  is estimated  $\tau$  is easily computed from  $\tan 2\tau = w_3/w_6$ . However, notice that the

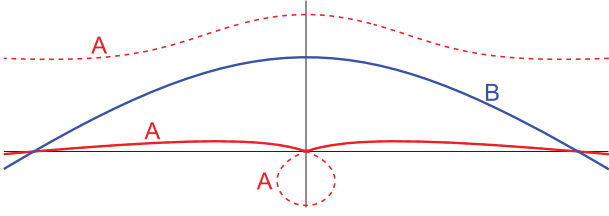


Fig. 4. Detail of two line projections A and B in a non-central catadioptric image with conical mirror. Line A (in red) pass through the singularity at the principal point (dotted points correspond to negative radius).

distance to the mirror  $Z_m$  is coupled with direction vector  $\mathbf{v}_l$  so it is not possible to separate them. Remember that when using the *inverse normalizing description*  $\|\mathbf{v}_l\|$  is the inverse of the minimal distance from the origin to the line. As  $\mathbf{v}_l$  and  $Z_m$  are coupled, it is possible to compute the inverse of the distance scaled by  $Z_m$  (The norm of the obtained vector  $\|\mathbf{v}_w\| = \rho_l Z_m$ ).

Because of this, we conclude that in conical catadioptric mirrors, if the distance of a conical mirror is unknown, it is not possible to reconstruct the scale of a scene only from line-images in a single image.

#### A. Parametric Description and Singularity

Expression (12) allows expressing  $r$  in terms of  $\theta$

$$r = \frac{-(\omega_4 \cos \theta + \omega_5 \sin \theta + \omega_6)}{\omega_1 \cos \theta + \omega_2 \sin \theta + \omega_3} \quad (15)$$

therefore, the parametric expression of the line-image curve becomes

$$x(\theta) = -(\omega_4 \cos \theta + \omega_5 \sin \theta + \omega_6) \cos \theta \quad (16)$$

$$y(\theta) = -(\omega_4 \cos \theta + \omega_5 \sin \theta + \omega_6) \sin \theta \quad (17)$$

$$z(\theta) = \omega_1 \cos \theta + \omega_2 \sin \theta + \omega_3. \quad (18)$$

In conical catadioptric systems the vertex cone projection ( $x = 0, y = 0$ ) is a singularity of line-images passing through it. If the line-image lies on this singularity, equation (15) returns negative values of  $r$  for some values of  $\theta$ . At the singularity, the curve is continuous but not derivable. Considering the points with negative radius the curve is derivable on the singularity. Actually, these points are not depicted on the catadioptric image (dotted points in Figure 4).

From equation (15) we can determine the range of values of  $\theta$  in which the radius is negative. The values of  $\theta$  limiting this range are computed from

$$\omega_4 \cos \theta + \omega_5 \sin \theta + \omega_6 = 0 \quad (19)$$

and solving for  $\tan \theta$  yields:

$$\tan \theta = \frac{-\omega_4 \omega_5 \pm \omega_6 \sqrt{\omega_4^2 + \omega_5^2 - \omega_6^2}}{\omega_5^2 - \omega_6^2}. \quad (20)$$

Notice that it does not exist real solution if the value inside the square root is negative. In other words, all  $\theta$  values (15) gives  $r > 0$  therefore the line-image does not belong to the singularity. So, we can state that a line-image pass through the discontinuity if and only if  $\omega_4^2 + \omega_5^2 > \omega_6^2$ .

## IV. ALGEBRAIC AND METRIC DISTANCES

When evaluating if a point belongs to a line-image or for fitting the curve is necessary a function measuring the distance from a point to the line-image. Depending on this distance the quality in precision of the extracted line-image is improved. In this paper we present a qualitative comparison among distances, some of them used in previous works, and we propose a metric distance on the normalized image plane as the natural space where data is acquired. In this section, we assume that coordinates on the normalized plane are  $(x, y, 1)^T$  instead the projective general case  $(x, y, z)^T$ .

Using (10) the algebraic distance

$$d_{alg} = Z_r (v_x y - v_y x) + (n_x x + n_y y) + n_z r \cot \phi \quad (21)$$

is measured in pixels when the Plücker lines are normalized with  $\|\mathbf{n}_l\| = 1$ . However this expression does not guarantee the metric conditions. As alternative we propose the point-to-point euclidean distance  $d_m(\mathbf{x}_1, \mathbf{x}_2) = \sqrt{(\mathbf{x}_1 - \mathbf{x}_2)^T (\mathbf{x}_1 - \mathbf{x}_2)}$  which satisfies the three metric conditions (no negativity, symmetry and triangle inequality).

Given a metric space  $(X, d_m)$  and  $L \subset X$  a subset of points lying on a line-image, the metric distance from a point  $\mathbf{x}$  to the line-image is:

$$d_m(\mathbf{x}, L) = \inf \{d_m(\mathbf{x}, \mathbf{x}_l) : \mathbf{x}_l \in L\} \quad (22)$$

Notice that in practice the point of the curve closer to the given point is the same using the Euclidean distance or the square Euclidean distance. By using the method of Lagrange multipliers it is possible to find the point  $\tilde{\mathbf{x}} = (\tilde{x}, \tilde{y})^T$  which minimizes the distance function

$$f_d(\tilde{\mathbf{x}}) = (\tilde{x} - x)^2 + (\tilde{y} - y)^2 \quad (23)$$

subject to the constraint  $g_l(\tilde{\mathbf{x}}) = 0$ .

Only a Lagrange parameter has to be computed and eliminating this parameter we finally obtain the equation system

$$\begin{aligned} h(\tilde{\mathbf{x}}) &= (\tilde{x} - x) \frac{\partial g_l}{\partial \tilde{y}} - (\tilde{y} - y) \frac{\partial g_l}{\partial \tilde{x}} = 0 \\ g_l(\tilde{\mathbf{x}}) &= 0. \end{aligned} \quad (24)$$

In other words, the point  $\tilde{\mathbf{x}}$  must satisfy lying on the line-image and the perpendicular straight line passing by this point must intersect  $\mathbf{x}$ .

To reach a close solution first we expand the compact line-image description (12) to get a polynomial expression, in this case a quartic.

$$g_l(\tilde{\mathbf{x}}) = r^2 (w_6 + w_1x + w_2y)^2 - (w_4x + w_5y + w_3r^2)^2 = 0 \quad (25)$$

where  $r^2 = x^2 + y^2$ .

The resulting polynomial  $h$  obtained from this expression is the quartic

$$(\tilde{x}^3, \tilde{x}^2\tilde{y}, \tilde{x}^2, \tilde{x}\tilde{y}^2, \tilde{x}\tilde{y}, \tilde{x}, \tilde{y}^3, \tilde{y}^2, \tilde{y}) \mathbf{W} \begin{pmatrix} \tilde{y} - y \\ x - \tilde{x} \end{pmatrix} = 0 \quad (26)$$

where

$$\mathbf{W} = \begin{pmatrix} 2w_1^2 - 2w_3^2 & w_1w_2 & w_1^2 + w_2^2 - 2w_3^2 \\ 3w_1w_2 & w_2w_6 - w_3w_5 & 3w_1w_2 \\ 3w_1w_6 - 3w_3w_4 & 2w_1w_6 - 2w_3w_4 & -w_4w_5 \\ w_1^2 + w_2^2 - 2w_3^2 & 2w_2^2 - 2w_3^2 & 2w_2^2 - 2w_3^2 \\ 2w_2w_6 - 2w_3w_5 & -w_4w_5 & 2w_2^2 - 2w_3^2 \\ w_6^2 - w_4^2 & w_1w_2 & 3w_2w_6 - 3w_3w_5 \\ w_1w_2 & w_1w_6 - w_3w_4 & w_6^2 - w_5^2 \\ w_1w_6 - w_3w_4 & -w_4w_5 & \end{pmatrix} \quad (27)$$

Computing the resultant between both equations from the variable  $\tilde{y}$  we obtain a single polynomial equation depending on  $\tilde{x}$  with degree 12.

$$(\tilde{x}^{12}, \tilde{x}^{11}, \tilde{x}^{10}, \tilde{x}^9, \tilde{x}^8, \tilde{x}^7, \tilde{x}^6, \tilde{x}^5, \tilde{x}^4, \tilde{x}^3, \tilde{x}^2, \tilde{x}, 1) \Omega \hat{x} = 0 \quad (28)$$

where  $\Omega(\omega) \in \mathbb{R}^{13 \times 15}$  and  $\hat{x} =$

$$(x^4, x^3y, x^3, x^2y^2, x^2y, x^2, xy^3, xy^2, xy, x, y^4, y^3, y^2, y, 1)^\top.$$

For a given point on the normalized plane  $(x, y)^\top$ , solving (28) results in 12 solutions for  $\tilde{x}$ . The correct solution can be found by checking  $g_l$  and  $h_l$  for each solution. From the remaining results we choose the one with minimal distance. Notice that  $\Omega$  only has to be computed for each line-image  $\omega$  whereas (28) is solved for each point.

In Figure 5 we show the different regions defined by a given threshold using three distances. First, we present Plücker distance which is the metric distance in 3D between rays and the given line. In this case the region defined by rays which are closer to a given distance to the line has a thickness in the image which is not constant. The algebraic distance given by the line-image also has variations in the thickness of the region when the line is close to the principal point. However the proposed metric distance on the image defines a region with an homogeneous thickness.

## V. EXPERIMENTS AND EVALUATION

In this section we show some examples of manual extraction using five points and we present quantitative results in the estimation of the mirror geometry from line-images.

We have used a conical mirror with a known  $\tau = 55 \text{ deg}$  by fabrication and an USB perspective camera. The system

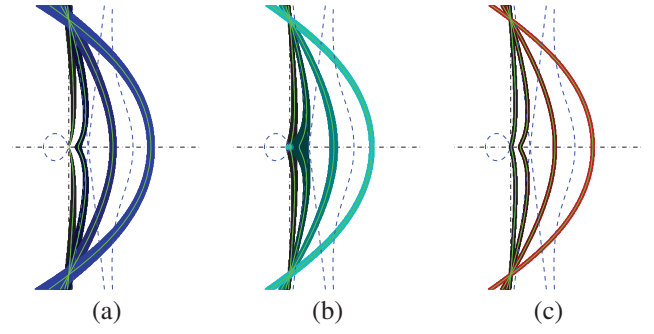


Fig. 5. Behaviour of the different metrics defined to decide if a point lies on a line-image for conical catadioptric systems. (a) Plücker distance. (b) algebraic distance in pixels. (c) metric distance. The thin lines are the actual line-images. The coloured region around the lines denotes the points of the region which have a distance minor than a threshold.

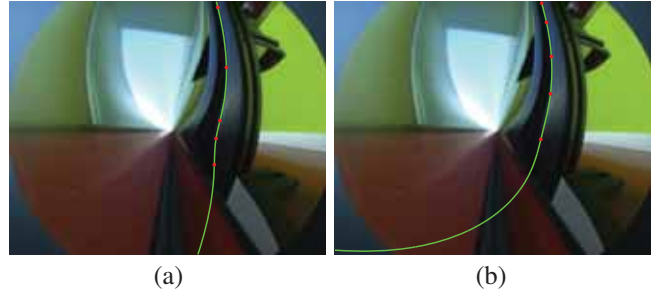


Fig. 6. Influence of points selection. (a) Good extraction (b) Bad Extraction. We can see the high influence of detected points in line extraction.

has been fixed manually to assure the alignment between the camera and the mirror therefore the vertex of the cone is projected in the center of the image. The perspective camera is calibrated independently using a standard method taking into account focal distance, principal point, skew and radial distortion. Small errors in the projection of the vertex of the cone are included in the principal point of the perspective model identifying manually the singularity of line-images. The distance  $Z_m$  is unknown and it is not necessary in this experiment.

Five points from conical catadioptric images (in red) are selected manually to compute the line-image  $\omega$  who is painted on the image using the parametric description (18). From each  $\omega$  line image we extract the Plücker coordinates of the line and the aperture angle of the mirror  $\tau$ . As explained in Section III the distance to the mirror  $Z_m$  is coupled with the Plücker coordinates therefore the metric in recovered 3D lines are scaled to this distance.

In Figure 6 we show the high influence of error and point selection. Depending on the selected points the extracted line-image fits or not the projected points of the line. In spite of both line-images are fitting the defining points and the rest of the projected point of the segment, the error in the estimation of the 4DOFs complicates the right extraction of the line. In Figure 7 we show some examples of line projections correctly extracted in different images and the obtained value for  $\tau$  in each one. We can see how this value is close to the ground truth which is  $\tau_{ref} = 55 \text{ deg}$ . Finally, in Figure 8 we show more examples of incorrect extractions. The reason of these

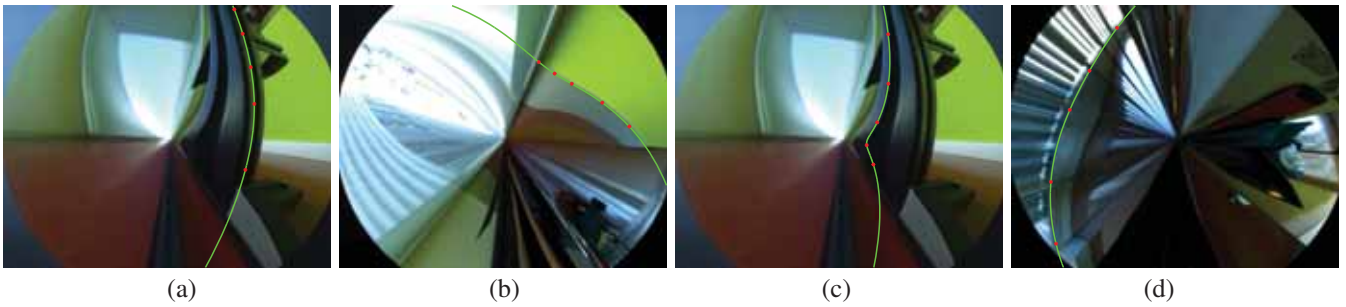


Fig. 7. Examples of correct extraction. (a)  $\tau = 55.0 \text{ deg.}$  (b)  $\tau = 55.5 \text{ deg.}$  (c)  $\tau = 56.1 \text{ deg.}$  (d)  $\tau = 54.9 \text{ deg.}$

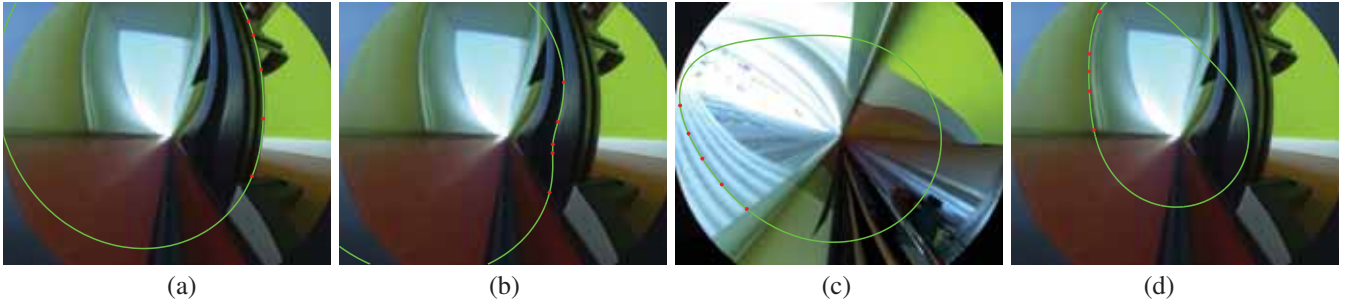


Fig. 8. Examples of incorrect extraction. (a)  $\tau = 50.9 \text{ deg.}$  (b)  $\tau = 51.1 \text{ deg.}$  (c)  $\tau = 49.7 \text{ deg.}$  (d)  $\tau = 48.4 \text{ deg.}$

errors is the sensitivity of line projection and the large number of degrees of freedom of the curve in non-central systems.

## VI. CONCLUSION

In this paper we investigate the geometry of line projections in conical catadioptric systems proposing a compact description of 6 homogeneous parameters for the line-image. This description explicitly shows the coupling between the distance from the camera to the mirror and the depth of a reconstructed line. Using the proposed parametrization the mirror aperture angle  $\tau$  can be computed from a single line-image. The proposal is tested with a real system with known geometry obtaining the projections of the line-images and an estimation of the aperture angle. However, supervision is still needed to select the defining points of a line. Future work will be focused in the robust automation of the process in order to provide a self-calibrating method.

## ACKNOWLEDGMENT

This work was supported by the Spanish project VINEA DPI2012-31781 and FEDER funds. First author was supported by the FPU program AP2010-3849. Thanks to Francisco Vasconcelos from the ISR-Coimbra for helping us tackling with the polynomial system of equations solving problem.

## REFERENCES

- [1] J. Bermudez-Cameo, L. Puig, and J. J. Guerrero, "Hypercatadioptric line images for 3D orientation and image rectification," *Robotics and Autonomous Systems*, vol. 60, no. 6, pp. 755 – 768, 2012.
- [2] A. Agrawal, Y. Taguchi, and S. Ramalingam, "Analytical forward projection for axial non-central dioptric and catadioptric cameras," in *European Conference on Computer Vision (ECCV 2010)*, pp. 129–143.
- [3] S. Teller and M. Hohmeyer, "Determining the lines through four lines," *Journal of graphics tools*, vol. 4, no. 3, pp. 11–22, 1999.
- [4] V. Caglioti and S. Gasparini, "On the localization of straight lines in 3D space from single 2D images," in *IEEE Computer Society Conference on Computer Vision and Pattern Recognition (CVPR 2005)*, vol. 1, pp. 1129–1134.
- [5] D. Lanman, M. Wachs, G. Taubin, and F. Cukierman, "Reconstructing a 3D line from a single catadioptric image," in *Third International Symposium on 3D Data Processing, Visualization, and Transmission*, 2006, pp. 89–96.
- [6] S. Gasparini and V. Caglioti, "Line localization from single catadioptric images," *International journal of computer vision*, vol. 94, no. 3, pp. 361–374, 2011.
- [7] C. Pinciroli, A. Bonarini, and M. Matteucci, "Robust detection of 3D scene horizontal and vertical lines in conical catadioptric sensors," in *Proc. 6th Workshop on Omnidirectional Vision*, 2005.
- [8] W. Chen, I. Cheng, Z. Xiong, A. Basu, and M. Zhang, "A 2-point algorithm for 3D reconstruction of horizontal lines from a single omnidirectional image," *Pattern Recognition Letters*, vol. 32, no. 3, pp. 524–531, 2011.
- [9] L. Perdigoto and H. Araujo, "Reconstruction of 3D lines from a single axial catadioptric image using cross-ratio," in *21th International Conference on Pattern Recognition (ICPR 2012)*, pp. 857–860.
- [10] V. Caglioti, P. Taddei, G. Boracchi, S. Gasparini, and A. Giusti, "Single-image calibration of off-axis catadioptric cameras using lines," in *International Conference on Computer Vision (ICCV 2007)*, pp. 1–6.
- [11] A. Agrawal and S. Ramalingam, "Single image calibration of multi-axial imaging systems," in *IEEE Computer Society Conference on Computer Vision and Pattern Recognition (CVPR 2013)*, pp. 1399–1406.
- [12] S. Baker and S. K. Nayar, *Single viewpoint catadioptric cameras*. Secaucus, NJ, USA: Springer-Verlag New York, Inc., 2001.
- [13] G. López-Nicolás and C. Sagüés, "Catadioptric camera model with conic mirror," in *British Machine Vision Conference (BMVC 2010)*.
- [14] P. Sturm, S. Ramalingam, J.-P. Tardif, S. Gasparini, and J. Barreto, *Camera models and fundamental concepts used in geometric computer vision*. Now Publishers, 2011.
- [15] J. Bermudez-Cameo, G. Lopez-Nicolas, and J. J. Guerrero, "A unified framework for line extraction in dioptric and catadioptric cameras," in *11th Asian Conference on Computer Vision, (ACCV 2012)*, vol. 7727.